Oxidative Damage of Mitochondrial Proteins Contributes to Fruit Senescence: A Redox Proteomics Analysis

ARTICLE *in* JOURNAL OF PROTEOME RESEARCH · MARCH 2009

Impact Factor: 4.25 · DOI: 10.1021/pr801046m · Source: PubMed

4 AUTHORS, INCLUDING:

Xianghong Meng
Ocean University of China
20 PUBLICATIONS **769** CITATIONS
SEE PROFILE

Qing Wang
Sun Yat-Sen University
54 PUBLICATIONS **1,471** CITATIONS
SEE PROFILE

Shiping Tian
Chinese Academy of Sciences
120 PUBLICATIONS **3,849** CITATIONS
SEE PROFILE

Article

Oxidative Damage of Mitochondrial Proteins Contributes to Fruit Senescence: A Redox Proteomics Analysis

Guozheng Qin, Xianghong Meng, Qing Wang, and Shiping Tian

J. Proteome Res., **2009**, 8 (5), 2449-2462• DOI: 10.1021/pr801046m • Publication Date (Web): 25 February 2009

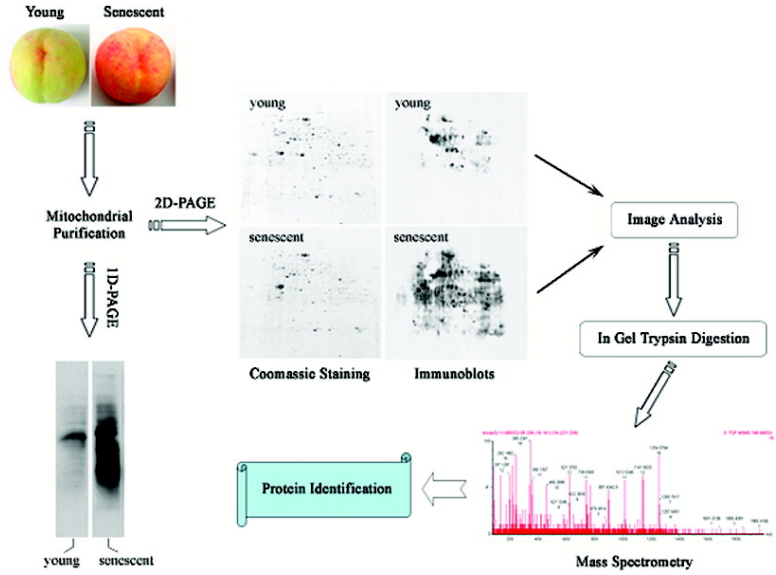

More About This Article

Additional resources and features associated with this article are available within the HTML version:

- Supporting Information
- Access to high resolution figures
- Links to articles and content related to this article
- Copyright permission to reproduce figures and/or text from this article

View the Full Text HTML

research articles Journal of proteome research

Oxidative Damage of Mitochondrial Proteins Contributes to Fruit Senescence: A Redox Proteomics Analysis

Guozheng Qin,‡ Xianghong Meng,‡ Qing Wang, and Shiping Tian*

Key Laboratory of Photosynthesis and Environmental Molecular Physiology, Institute of Botany, Chinese Academy of Sciences, Beijing 100093, China

Received December 5, 2008

Oxidative damage to mitochondria caused by reactive oxygen species (ROS) has been implicated in the process of senescence as well as a number of senescence-related disorders in a variety of organisms. Whereas mitochondrial DNA was shown to be oxidatively modified during cellular senescence, mitochondrial protein oxidation is not well-understood. With the use of high-resolution, two-dimensional gel electrophoresis coupled with immunoblotting, we show here that protein carbonylation, a widely used marker of protein oxidation, increased in mitochondria during the senescence of peach fruit. Specific mitochondrial proteins including outer membrane transporter (voltage-dependent anion-selective channel, VDAC), tricarboxylic acid cycle enzymes (malate dehydrogenase and aconitase), and antioxidant proteins (manganese superoxide dismutase, MnSOD) were found as the targets. The oxidative modification was concomitant with a change of VDAC function and loss of catalytic activity of malate dehydrogenase and MnSOD, which in turn facilitated the release of superoxide radicals in mitochondria. Reduction of ROS content by lowering the environmental temperature prevented the accumulation of protein carbonylation in mitochondria and retarded fruit senescence, whereas treatment of fruit with H_2O_2 had the opposite effect. Our data suggest that oxidative damage of specific mitochondrial proteins may be responsible for impairment of mitochondrial function, thus, leading to fruit senescence. Proteomics analysis of mitochondrial redox proteins provides considerable information on the molecular mechanisms involved in the progression of fruit senescence.

Keywords: mitochondria • reactive oxygen species • senescence • protein oxidation • redox proteomics

Introduction

Fruits are developmental structures that are exclusive to flowering plants and play a central role in seed maturation and dispersal.[1] The rich nutrients contained in fleshy fruits such as flavor compounds, fiber, vitamins, and antioxidants make fruits an important component of human diets.[2] Senescence is a vital aspect of fruit production with direct impact for our food supply, nutrition, and health. Thus, unraveling the molecular and biochemical basis of fruit senescence has biological and dietary significance. Fruit senescence is regulated by various internal and environmental factors including developmental signals and genes, hormones, light and temperature.[2−5] Large numbers of studies have focused on the crucial role of ethylene,[2,6,7] whereas it has become clear that many types of fruits do not require increased ethylene biosynthesis in this process.[8] Discovering the common regulatory mechanisms shared by all types of fruits would create new opportunities for controlling fruit senescence.[8] It has been demonstrated that fruit senescence was an oxidative phenomenon which required a pronounced increase in reactive oxygen species (ROS), such as H_2O_2 and superoxide anion.[9−11] However, the detailed mechanisms underlying the regulatory effects of ROS in the process of fruit senescence remain largely unknown. According to the 'free radical theory of aging',[12] oxidative damage to biological macromolecules contributes to the irreversible, deleterious changes of biological systems. The generation of ROS and the degree to which they cause oxidative injury play important roles in the progression of senescence and various senescence-associated disorders.[13]

Mitochondria are a primary generator of endogenous ROS. Therefore, mitochondrial components are particularly vulnerable to oxidative damage and mitochondria have become a major focus of research in the area of senescence.[14−17] A number of biochemical functions are performed by mitochondria, among which the primary roles are the oxidation of organic acids through the tricarboxylic acid cycle and the synthesis of ATP.[18] Functional integrity is required for mitochondria to meet cellular energy demands. Impairment of mitochondrial function caused by oxidative damage to mitochondrial DNA, lipids and proteins has been implicated during various pathophysiological states associated with oxidative stress and senescence.[19,20] Mitochondrial DNA is highly susceptible to oxidative damage because it is located close to the inner mitochondrial membrane, where the ROS are generated.

* To whom correspondence should be addressed. Prof. Shiping Tian, Key Laboratory of Photosynthesis and Environmental Molecular Physiology, Institute of Botany, Chinese Academy of Sciences, 20 Nanxincun, Xiangshan, Haidian District, Beijing 100093, China. Tel.: 0086-10-62836559. Fax: 0086-10-82594675. E-mail: tsp@ibcas.ac.cn.

‡ These authors contributed equally to this work.

10.1021/pr801046m CCC: $40.75

Published on Web 02/25/2009

In addition, mitochondrial DNA is small in size and is not protected by histone proteins as is the case for nuclear DNA. Thus, oxidative damage to mitochondrial DNA has been intensively studied during the process of senescence.[21−24] By contrast, the correlation between mitochondrial protein oxidation and cellular senescence is not well-understood,[25] although it has been realized that specific mitochondrial proteins are susceptible to oxidative damage.[26,27] Oxidation of sensitive proteins can significantly affect their biochemical characteristics such as enzyme activities, structural functions, and susceptibility to proteolysis.[28,29] Accumulating evidence suggests that there is a direct correlation among increased levels of protein oxidation and process of cellular deterioration.[30−32] Among a variety of methods for assessing protein oxidative damage, protein carbonylation has been used extensively.[33] Carbonylated proteins can be formed by direct oxidation of amino acid side chains or via indirect reactions with lipid peroxidation products.[34] Histidine, arginine, and lysine are the most susceptible amino acids for this process.

With the advent of proteomics and mass spectrometry (MS), it becomes possible to identify the specific proteins that are susceptible to undergo oxidative modifications.[35] An approach of functional proteomics, namely, redox proteomics, has been employed by coupling two-dimensional (2D) gel electrophoresis with immunoblotting which focuses on carbonylated proteins. Such an approach provides a powerful tool to study a family of proteins with the same post-translational modification such as carbonylation.[36] In a previous study to screen the oxidized proteins in the matrix of rice leaf mitochondria, Kristensen et al.[37] identified 20 oxidized proteins in the untreated sample and a further 32 in the oxidized sample. The authors concluded that a group of mitochondrial proteins are particularly susceptible to oxidative stress, but the deleterious effect of carbonylation on protein characteristics and the consequence for plant growth and development were not determined. The present studies investigated the effects of mitochondrial protein oxidation during the progression of fruit senescence. Mitochondria were isolated from peach fruit in high purity by Percoll density gradient centrifugation. To gain a better understanding of the relationship among ROS production, mitochondrial protein carbonylation, and process of senescence, fruits were placed under low temperature, which would decrease ROS content and retard senescence, or treated with hydrogen peroxide to induce oxidative stress. Since carbonylation might change protein properties, we also analyzed the biological functions of the main protein targets. Our data demonstrate that oxidative damage of specific mitochondrial proteins caused by ROS results in the dysfunction of protein targets, which in turn facilitates further release of ROS and enhances mitochondrial protein oxidation, eventually leading to the onset of fruit senescence. These results provide novel insights into the regulatory effect of ROS on fruit senescence.

Materials and Methods

Plant Material, Mitochondria Isolation, and Purity Assessment. Peach (*Prunus persica* L. Batsch) fruits were detached at commercial maturity from trees. Fruit on the day of harvest was regarded as young, while fruit placed under room temperature for 12 days was used as senescent. We used detached fruits as a model to study the molecular mechanisms of fruit senescence because the onset of senescence in these tissues can be strictly regulated. In addition, detached fruits function as independent organs and are free of metabolic interactions with other plant parts. Since respiration is the predominant process in the life of the detached fruit, it offers desirable material for investigation of mitochondrial systems in the progression of fruit senescence.

Mitochondria were isolated as described by Moreau and Romani[38] and Taylor et al.[39] with all steps performed at 4 °C. Peaches were peeled and 130 g of tissues was homogenized with a Warring blender in 390 mL of ice-cold extraction medium containing 250 mM sucrose, 1 mM EDTA, 0.5% (w/v) polyvinylpyrrolidone-40, 0.1% (w/v) BSA, 10 mM β-mercaptoethanol, and 50 mM Tris-HCl, pH 7.5. The pH value was kept between 7.0 and 7.1 during homogenization with dropwise additions of 1 N KOH. After filtering homogenate through four layers of sterile cheesecloth, the filtrate was centrifuged for 15 min at 1200*g*. The supernatant was collected and centrifuged for 20 min at 17 000*g*. The resultant organelle pellet was kept and resuspended in wash buffer (250 mM sucrose, 0.1% (w/v) BSA, and 50 mM Tris-HCl, pH 7.5) with a soft, small brush. Mitochondria were subsequently purified by layering on top of a step Percoll gradient at 8, 12, and 30% (2:4:1) in wash buffer and centrifuged for 45 min at 40 000*g*. The mitochondria layer at the interface of the heaviest and the middle gradient densities was aspirated and washed by centrifugation for 15 min at 15 000*g* with wash buffer. To further purify the mitochondria, concentrated mitochondria was loaded onto a self-generated 21% (v/v) Percoll gradient and centrifuged for 30 min at 40 000*g*. The mitochondrial bands which were enriched close to the middle of the gradient were aspirated and washed twice with wash buffer to remove Percoll by centrifugation for 15 min at 15 000*g*. The purity of mitochondria was evaluated (Supplemental Figure 1 in Supporting Information) following the methods of Millar et al.[40]

Determination of Fruit Firmness and Hydrogen Peroxide Content. The firmness of fruit was determined by a penetrometer (FT-327, UC Fruit Firmness Tester, Milano, Italy) following the method of Cantu et al.[41] Fruits were measured at two sites, and 10 fruits were used at each time interval. Content of H_2O_2 was determined according to the method described by Ding et al.[42] Samples containing 10 g of flesh were homogenized with 20 mL of ice-cold acetone using a polytron tissue grinder (Kinematica CH-6010, Brinkman Co., Kriens-Luzern, Switzerland) at 4 °C. The mixture was centrifuged at 17 000*g* for 40 min at 4 °C, and the supernatant was collected. Titanyl sulfate at 50 g L^{-1} and concentrated NH_4OH solution were added to precipitate the peroxide−titanium complex. After centrifugation at 6000*g* for 5 min, the supernatant was discarded and the pellet was washed three times with cold acetone. The precipitate was then dissolved in 2 N of sulfuric acid and immediately used for H_2O_2 determination at 415 nm. The H_2O_2 content was calculated from a standard curve prepared with known amounts of H_2O_2 in a similar way and expressed as micromole per gram (μmol g^{-1}) of fresh weight.

Retard Fruit Senescence and Induce Oxidative Stress. To retard senescence, fruits were placed for 12 days under low temperature (0 °C), which has been used extensively to delay senescence of peach fruits.[43,44] To induce oxidative stress, fruits were immersed in 100 mM H_2O_2 solution for 20 min and placed under room temperature. The concentration of H_2O_2 was selected based on an initial screen, in which H_2O_2 at 100 mM was effective to induce oxidative stress without apparent injury to the fruit epidermis. Fruits were used for mitochondria isolation or biochemical analysis after 12 days of incubation.

SDS-PAGE of DNP-Derivatized Mitochondrial Proteins. For protein extraction, purified mitochondria were lysed by sonication on ice in 1 mL of lysis buffer containing 50 mM Tris-HCl (pH 7.2), 2% (v/v) β-mercaptoethanol, and 1 mM PMSF. The homogenate was centrifuged (25 000*g*, 20 min; 4 °C) and proteins in the supernatant were precipitated for 30 min at 4 °C with ice-cold trichloroacetic acid at final concentration of 10% (w/v). The protein pellets were collected by centrifugation at 25 000*g* for 20 min at 4 °C and washed three times with cold acetone to remove remaining trichloroacetic acid. The mitochondrial proteins were finally solubilized in sample buffer consisting of 7 M urea, 2 M thiourea, 4% (w/v) CHAPS, 1% (w/v) dithiothreitol, and 2% (v/v) carrier ampholytes (pH 3−10). Protein concentration was determined by the method of Bradford.[45]

Mitochondrial carbonylated proteins were measured with the OxyBlot Protein Oxidation Detection Kit (Chemicon International, Billerica, MA) according to the manufacturer's specifications. Samples containing 30 μg of proteins were added to an equal volume of 12% SDS. Protein carbonyl groups were then derivatized to 2,4-dinitrophenylhydrazone (DNP) by incubation with 1 additional vol of 2,4-dinitrophenylhydrazine (DNPH) for 15 min at room temperature. The reaction was stopped by the addition of 1 vol of neutralization solution. Derivatized protein samples were separated by 12% SDS-PAGE and transferred to PVDF membrane (Millipore Corp., Billerica, MA) using a TE 77 semidry transfer unit (GE Healthcare Bio-Sciences AB, Uppsala, Sweden). The oxidatively modified proteins were detected with anti-DNP antibodies (anti-dinitrophenyl-group antibodies) and a secondary horseradish peroxidase-conjugated antibody. A chemiluminescence detection kit (SuperSignal, Pierce Biotechnology, Rockford, IL) was used to visualize the immunoreactive bands. To monitor the equal loading of samples, colloidal Coomassie Brilliant Blue (CBB) R-250 was used to stain the proteins in the gels.

Two-Dimensional Gel Electrophoresis of Carbonylated Mitochondrial Proteins. Two-dimensional (2D) gel electrophoresis of carbonylated proteins was carried out according to the method of Dirmeire et al.[46] with some modifications. Aliquots of 600 μg of mitochondrial proteins resolved in 250 μL of sample buffer (7 M urea, 2 M thiourea, 4% (w/v) CHAPS, 1% (w/v) dithiothreitol, 2% (v/v) carrier ampholytes (pH 3−10), and 0.001% (w/v) bromphenol blue) were applied to rehydrate gel strips with an immobilized nonlinear pH gradient from 3 to 10 (Immobiline DryStrip pH 3−10 NL, 13 cm; GE Healthcare Bio-Sciences AB). The strips were rehydrated overnight and then the first-dimensional IEF was performed at 20 °C for a total of 20 kVh on an Ettan IPGphor unit (GE Healthcare Bio-Sciences AB) following the manufacturer's instruction. Following IEF, the proteins in the Immobiline strips were derivatized by incubating in a solution of 10 mM DNPH for 20 min at room temperature with gentle agitation. The strips were then transferred and incubated for 10 min in each of the following solutions: (1) 150 mM Tris-HCl, pH 6.8, 8 M urea, 20% (v/v) glycerol, and 2% (w/v) SDS; (2) 150 mM Tris-HCl, pH 6.8, 8 M urea, 20% (v/v) glycerol, 2% (w/v) SDS, and 1% (w/v) DTT; and (3) 150 mM Tris-HCl, pH 6.8, 8 M urea, 20% (v/v) glycerol, 2% (w/v) SDS, 4% (w/v) iodoacetamide, and a trace amount of bromophenol blue. SDS-PAGE in the second dimension was conducted using 15% polyacrylamide gels with 5% stacking gels. The Immobiline strips were placed on top of the stacking gels and sealed with a solution of 0.5% (w/v) agarose. Electrophoretic separation was conducted at a constant 30 mA per gel in a running buffer containing 25 mM Tris (pH 8.3), 195 mM glycine, and 0.1% (w/v) SDS. After electrophoresis, proteins were visualized by CBB R-250 or transferred to PVDF membrane and detected with anti-DNP antibodies as described above.

Image Analysis. Image analysis was carried out as described by Sultana et al.[32] The CBB stained gels and PVDF membranes were scanned using a flatbed scanner (GE Healthcare Bio-Sciences AB) and saved in TIF format. Image Master 2D Elite software (GE Healthcare Bio-Sciences AB) was used to compare protein expression and protein oxidation in the 2D gel images and 2D blots, respectively, between samples. To account for experimental variation, at least three biological repeats were used for either gels or blots of each sample. The amount of a protein spot was calculated based on the volume of that spot. To reflect the quantitative variations in intensity between different samples, the spot volume was normalized as a percentage of the total protein on gel or oxidized protein on blot. The spot intensity values obtained on the 2D blots were divided by the spot intensity value on the gels to get the level of specific protein carbonyls. The minimum requirement for spot quantification was spot presence in at least three biological replicates for either gels or blots. Statistical analysis of the data was performed using SPSS software (SPSS, Inc., Chicago, IL). A two-tailed nonpaired Student's *t*-test was used to determine whether the relative change was statistically significant between samples. Protein spots whose levels of carbonylation on average increased by at least 1.5-fold were excised for protein identification.

In-Gel Digestion, Mass Spectrometry, and Database Searching. In-gel digestion was performed following our previous reports.[47] Briefly, Coomassie blue stained protein spots were cut from the gels and destained with 50 mM NH_4HCO_3 in 50% (v/v) methanol for 1 h at 40 °C. Gel particles were mixed with 10 mM DTT in 100 mM NH_4HCO_3 for 1 h at 60 °C to reduce the proteins. To alkylate the proteins, the gels were dried in a vacuum centrifuge for 30 min prior to incubating with 40 mM iodoacetamide in 100 mM NH_4HCO_3 for 30 min at ambient temperature in the dark. Then, the gel pieces were washed several times with water and completely dried in a vacuum centrifuge. Enzymatic digestion was performed by adding gel pieces into the digestion buffer containing 100 mM NH_4HCO_3 and 5 ng/μL trypsin. The reaction mixture was incubated at 37 °C for 16 h. Digested peptides were extracted with three changes of 0.1% trifluoroacetic acid (TFA) in 50% acetonitrile. Solutions were collected and concentrated to 10 μL, and then desalted with ZipTipC_{18} (Millipore Corp.). Peptides were eluted from the column in 2 μL of 0.1% TFA in 50% acetonitrile.

Tandem Electrospray ionization mass spectrometry (ESI-MS/MS) was performed with a quadrupole time-of-flight mass spectrometer (Q-TOF-2; Micromass, Altrincham, U.K.), equipped with a z-spray source as described previously.[47] The instrument was externally calibrated using the fragmentation spectrum of the doubly charged 1571.68 Da (785.84 m/z) ion of fibrinopeptide B before loading the digested peptide samples. The peptides were loaded by nanoelectrospray using gold-coated borosilicate glass capillaries (Micromass). The capillary voltage was set to an average of 1000 V, and the sample cone to 50 V. Dependent on the mass and charge state of the peptides, the collision energy was varied from 14 to 40 V. Peptide precursor ions were acquired over the m/z range 400−1900 Da in TOF-MS mode. Multiply charged (2+ and 3+) ions rising above predefined threshold intensity were automatically selected for

MS/MS analysis, and product ion spectra collected from m/z 50−2000. To create peak lists, ProteinLynx (version 4.0; Micromass) was used with default parameter settings to process the tandem MS data. The generated peak lists were uploaded to Mascot MS/MS Ions Search program (version 2.1) on the Matrix Science (London, U.K.) public Web site (http://www.matrixscience.com) and protein identification was performed against NCBInr protein databases (version 20080314; 6 307 426 sequences and 2 155 784 383 residues) with a taxonomy restriction to 'Viridiplantae (Green Plants)'. Trypsin was chosen as the proteolytic enzyme, and one missed cleavage was permitted. Fixed modification was not selected and variable modifications included carbamidomethylation of cysteine, oxidation of methionine, and N-terminal pyroglutamine. Precursor and fragment ion mass tolerances were set to 1.2 and 0.6 Da, respectively. Peptide charge of +2 and +3 and monoisotopic mass was chosen, and the instrument type was set to ESI-QUAD-TOF. A total of 475 788 sequences in the database were actually searched. Only significant hits as defined by Mascot probability analysis were considered. Mascot uses a probability-based "Mowse score" to evaluate data obtained from tandem mass spectra. Mowse scores were reported as $-10 \times \mathrm{Log}_{10}(p)$ where p is the probability that the observed match between the experimental data and the database sequence is a random event. Mowse scores greater than 46 were considered significant ($p < 0.05$) and the best match is the one with the highest score. Protein identification was based on at least three distinct peptides. For proteins that were identified with MS/MS spectra matched to less than three peptides, MS/MS spectra were subjected to *de novo* sequence analysis using PEAKS Version 4.5 software (www.bioinformaticssolutions.com). The generated peptide sequences were used for homology searching using online tools (MS BLAST, EMBL, http://dove.embl-heidelberg.de/Blast2/msblast.html) as described by Shevchenko et al.[48] with the default search settings and the nrdb95 database (Supplemental Table 1 in Supporting Information). If only one matching peptide was found, nearly complete Y-ion series and partial complementary B-ion series needed to be present as determined by manual inspection. Information for single-peptide-based identifications is provided as Supplemental Table 2 in Supporting Information. To eliminate the redundancy of proteins that appeared in the database under different names and accession numbers, the single-protein member belonging to the species Prunus or else with the highest protein score (top rank) was singled out from the multiprotein family. If protein isoforms were observed, these entries were inspected manually and the presence of each protein isoform was confirmed by the identification of at least two unique peptides.

NADH Oxidation and Ultrastructural Analysis. The NADH oxidation in the mitochondria was measured following the method of Yagoda et al.[49] by monitoring the decrease in absorbance at 340 nm (typically by recording at 5-s intervals). Purified mitochondria were resuspended in R-buffer (0.65 M sucrose, 10 mM HEPES (pH 7.5), 10 mM KH_2PO_4, 5 mM KCl, 5 mM $MgCl_2$) to a final concentration of 100 mg mL^{-1}. About 30 mM NADH (final concentration) was added and the absorbance was monitored over a 35 min period. The absorbance was converted to NADH concentration by dividing it with the molar extinction coefficient (6.22×10^3 mM^{-1} cm^{-1}).

For transmission electron microscopy, the specimens were cut into smaller block about 4 mm^3 with a razor blade and fixed in 2.5% glutaraldehyde in PBS for 2 h. After washing with PBS, the specimens were incubated in 1% osmium tetraoxide in the same buffer for 12 h at 4 °C. Then, the samples were rinsed and dehydrated in a graded acetone series and embedded in Spurr's resin. Ultrathin sections about 70 nm stained with uranyl acetate and lead citrate were observed at 80 kV with a JEOL 1230 electron microscope (Kyoto, Japan).

Determination of Superoxide Anion Content in Mitochondria. Superoxide anion (O_2^-) content in mitochondria was determined following the method described by Oracz et al.[33] with minor modification. Purified mitochondria were resuspended in sodium phosphate buffer (pH 7.8, 50 mM) and lysed by sonication on ice. Unbroken mitochondria were removed by centrifugation at 16 000g for 20 min at 4 °C and the supernatants were used for O_2^- measurement. The supernatant was first incubated with 1 mM hydroxylamine hydrochloride in sodium phosphate buffer (pH 7.8, 50 mM) for 30 min at 25 °C. Then, 4-aminobenzenesulfonic acid at 17 mM and α-naphthylamine at 7 mM was added and the reaction mixture was incubated for 30 min at 25 °C. After centrifugation at 15 000g for 10 min, the absorbance was measured at 540 nm with a spectrophotometer (UV-160; Shimadzu Corp., Kyoto, Japan). A calibration curve was established using sodium nitrite and the content of O_2^- was expressed as nanomole per milligram (nmol/mg) of protein.

Enzyme Activity Assay. For enzyme analysis, purified mitochondria were lysed as indicated above. Manganese superoxide dismutase (MnSOD) activity was analyzed according to the method of Jakubowski et al.[50] In the assay, superoxide ions, generated by reaction of xanthine oxidase with xanthine, convert NBT to NBT-diformazan, which absorbs light at 560 nm. SOD reduces the superoxide ion concentration and thereby lowers the rate of NBT-diformazan formation. MnSOD activity was obtained by subtracting CuZn-SOD activity from the total activity. The specific activity was expressed as units per milligram (U/mg) of protein, where 1 unit was defined as the amount of the enzyme resulting in a 50% decrease of the formation of NBT-diformazan.

Aconitase activity was determined spectrophotometrically by monitoring the disappearance of *cis*-aconitate ($\varepsilon_{240} = 3.6$ mM^{-1} cm^{-1}) at 240 nm for 15 min.[51] Activity was expressed as milliunits per miligram (mU/mg) of protein. One milliunit was defined as the amount of enzyme that converted 1 nmol *cis*-aconitate per minute.

Activity of malate dehydrogenase was assayed by following the reduction of NAD, measured by the absorbance change at 340 nm.[52] The mitochondrial extract was incubated with sodium L-malate (100 mM), This-HCl (100 mM, pH 9), and NAD (2.5 mM). Results were expressed as milliunits per milligram (mU/mg) of protein, where 1 mU was defined as 1 nmol NADH ($\varepsilon_{340} = 6.22 \times 10^3$ mM^{-1} cm^{-1}) formed per minute.

Results

Oxidative Modification of Mitochondrial Proteins during Natural Senescence. Peach fruit softened quickly during natural senescence, accompanied by the alteration of pericarp color from green to red (Figure 1A). As related to the changes in softening (Figure 1B) and pericarp color, the hydrogen peroxide (H_2O_2) content enhanced significantly (Figure 1C). The increase of H_2O_2 has been reported during senescence of various fruits including pears, tomato, and muskmelons.[9−11] To determine whether ROS production could be associated with mitochondrial protein carbonylation, immunochemical detection was performed using anti-DNP (anti-dinitrophenyl-group) antibodies after one-dimensional (1D) gel electrophoresis. As indicated

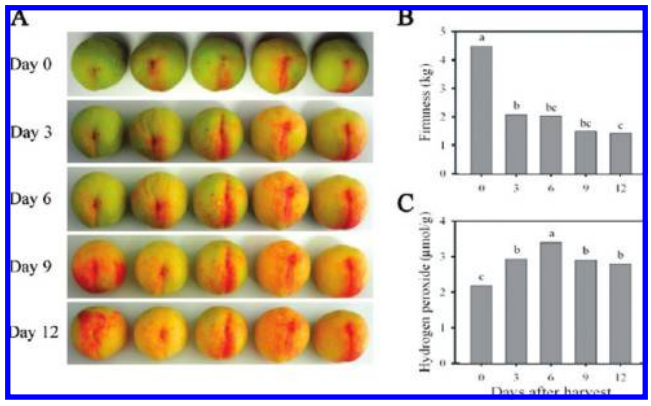

Figure 1. Changes of hydrogen peroxide content during natural fruit senescence. Fruit were detached at commercial maturity and placed under room temperature. (A) Images of fruit taken at day 0, 3, 6, 9, and 12. (B) Measurement of fruit softening during fruit senescence. (C) Hydrogen peroxide content assayed spectrophotometrically. Bars with different letters are significantly different from each other by the least significant difference test ($p < 0.05$).

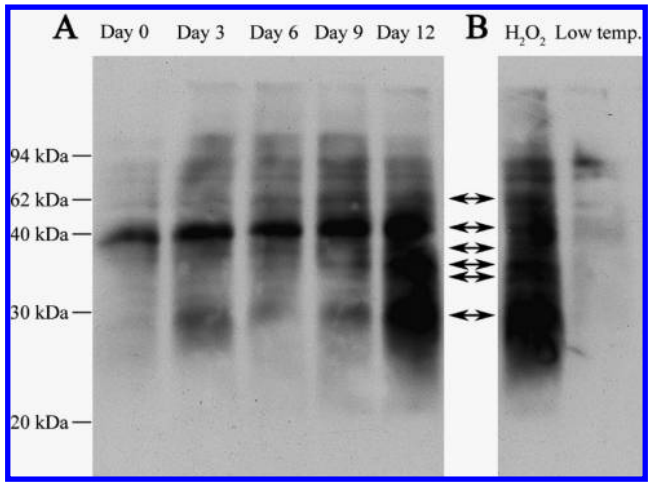

Figure 2. One-dimensional gel electrophoresis of carbonylated mitochondrial proteins. Mitochondrial proteins were separated by SDS-polyacrylamide gel electrophoresis. For immunodetection of carbonylated mitochondrial proteins, proteins were transferred to PVDF membrane and detected with anti-dinitrophenyl-group antibodies. (A) Carbonylation of mitochondrial proteins in fruit during natural senescence at days as indicated. (B) Carbonylation of mitochondrial proteins from fruit treated with H_2O_2 or under low temperature. The arrows indicate protein bands that are highly carbonylated.

in Figure 2A, multiple mitochondrial protein bands were selectively modified during the process of fruit senescence, suggesting that mitochondrial proteins are especially sensitive to oxidative damage. These proteins ranged in sizes with apparent molecular masses from 30 to 60 kDa. Application of H_2O_2 enhanced the carbonylation levels of mitochondrial proteins, whereas lowering the environmental temperature had the opposite effect (Figure 2B).

To identify specific targets for protein carbonylation, we subjected mitochondrial proteins to high-resolution 2D gel electrophoresis followed by immunochemical detection of carbonylated proteins. A schematic showing the methods used is shown in Supplemental Figure 2 in Supporting Information. Comparisons of protein expression and protein oxidation between samples were performed in 2D gels and 2D blots, respectively. The level of specific protein carbonyls was normalized to the protein content in the 2D gel by dividing the carbonyl level of a protein spot on the PVDF membrane by the protein level of its corresponding protein spot on the gel. Average ratios of specific carbonylation levels between samples were calculated from three biological repeat experiments. Consistent with the data obtained by 1D gel electrophoresis (Figure 2A), some proteins (94 proteins) showed a dramatic increase in protein carbonylation in senescent fruit (12 days after harvest) compared to newly harvested young fruit (0 day after harvest) (Figure 3B,D). For protein identification, 41 protein spots with relatively high abundance were excised from Coomassie stained gel and subjected to MS/MS analysis after in-gel trypsin digestion. Of these proteins, 11 had no MS/MS data, whereas two did not fit with the database. Their identities need to be further confirmed. Table 1 summarizes the mitochondrial proteins identified in our study which exhibited a significant increase in specific protein carbonylation levels during fruit senescence as assessed by the Student's *t*-test (see column titled "senescent vs young"). Of these, four are tricarboxylic acid (TCA) cycle related enzymes, including NAD-dependent malate dehydrogenase (spot 51), NADP-dependent malic enzyme (spot 11), 2-oxoacid dehydrogenase family protein (spot 14), and pyruvate decarboxylase (spot 12). Three protein spots (spots 46, 47, and 78) were identified as the same protein, mitochondrial voltage-dependent anion-selective channel (VDAC) or porin, which belongs in the mitochondrial outer membrane. Their location in the gels differed slightly in molecular mass and isoelectric point, indicating that they might be isoforms. Spot 1 was identified as heat shock protein 70 (HSP70) and spot 59 as manganese superoxide dismutase (MnSOD); both proteins are involved in oxidative stress responses. The influence of oxidative modification on the function of these proteins was analyzed in the subsequent studies. Of the remaining proteins, two are enzymes involved in carbon (enoyl-CoA hydratase [spot 40]) and nitrogen (gamma-aminobutyrate transaminase [spot 37]) metabolism. The other proteins were glutathione *S*-transferase (spot 63), annexin (spot 83), 14-3-3 family protein (spot 28), hydrogen ion transporting ATP synthase (spot 3), glyceraldehyde-3-phosphate dehydrogenase (spot 86), and enolase (spot 94). The presence of these proteins within the mitochondrial fraction may represent contamination from the mitochondrial purification process, or alternatively, these proteins may distribute in both mitochondria and cytosol as fumarase.[53] Besides identified proteins, several spots (spots 15, 24, 27, 36, and 60) had no MS/MS data or did not match with the database. The MS/MS peptide sequence of the identified proteins is summarized in Supplemental Table 3 in Supporting Information.

Mitochondrial Protein Carbonylation under Low Temperature or Hydrogen Peroxide Stress. To assess a putative causal association between ROS production, mitochondrial protein oxidation and fruit senescence, fruits were placed under low temperature, a practice used extensively to retard fruit senescence. Low temperature delayed fruit softening and reduced the production of H_2O_2 (Supplemental Figure 3 in Supporting Information). After leaving the fruits at 0 °C for 12 days, mitochondria were purified. Proteins were separated by 2D electrophoresis followed by immunoblotting using anti-DNP antibodies. As shown in Figure 4B, protein carbonylation in fruit under low temperature showed similar pattern as that in the newly harvested young fruit. The fold change of specific

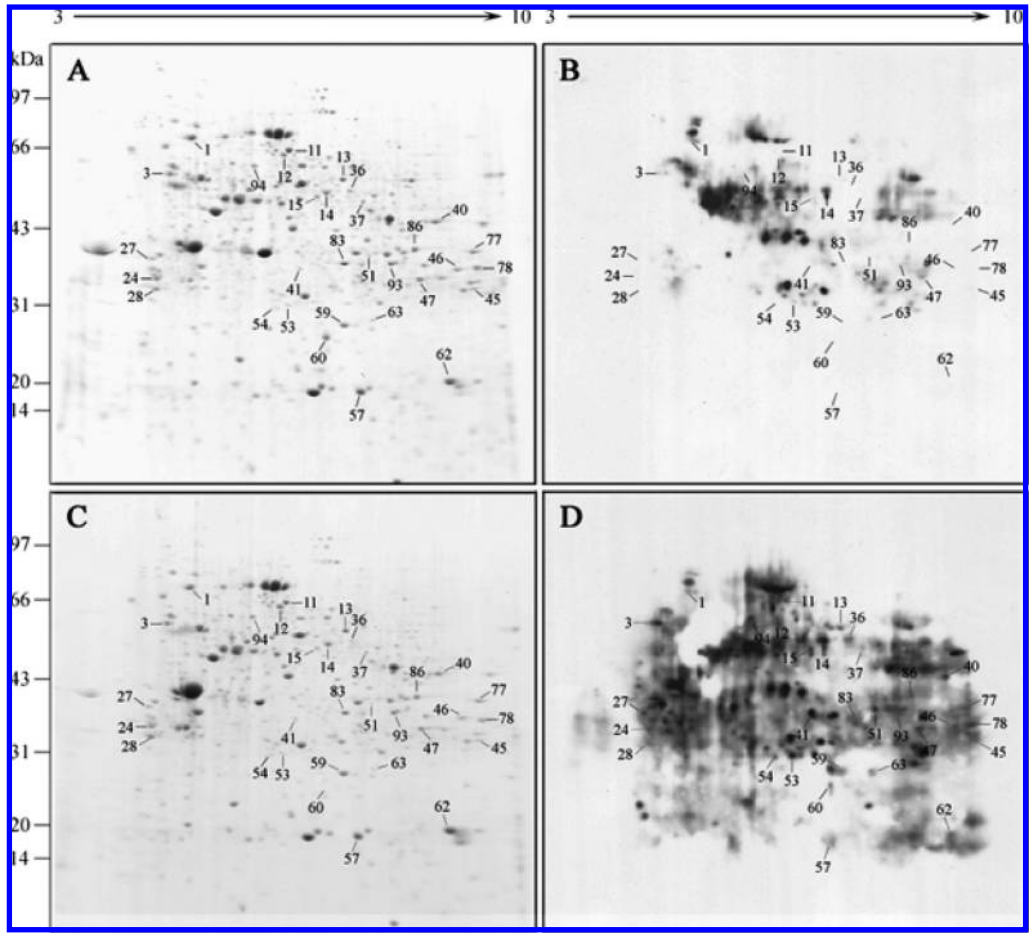

Figure 3. Two-dimensional (2D) immunoblots of carbonylated mitochondrial proteins during natural fruit senescence. Mitochondria were isolated from young (A and B) and senescent fruit (C and D). Mitochondrial proteins were separated by 2D gel electrophoresis using 13 cm Immobiline Drystrip with a pH 3−10 nonlinear gradient. After electrophoresis, proteins were visualized by Coomassie blue staining (A and C) or transferred to PVDF membrane for immunoblot analysis with anti-dinitrophenyl-group antibodies (B and D). Those proteins with increased levels of carbonylation in senescent fruit are indicated on both the protein stains and immunoblots. Numbers correspond to the proteins that have been identified by mass spectrometry (listed in Table 1).

protein carbonylation levels between fruit under low temperature and young fruit is summarized in Table 1 (see column titled "low temp. vs young"). To further document the correlation between fruit senescence, ROS accumulation and the carbonylation of mitochondrial proteins, fruits were treated with 100 mM of H_2O_2 solution. After this treatment, the internal H_2O_2 content was increased and the fruit were more susceptible to fungal pathogens (Supplemental Figure 4 in Supporting Information), suggesting H_2O_2 could accelerate fruit senescence.[41] Results of 2D immunoblotting indicated that more proteins appeared to be oxidized in response to H_2O_2 application and the intensity of immunostaining of some proteins increased dramatically (Figure 4D). These results are consistent with the pattern in 1D immunoblotting (Figure 2B), which indicated that low temperature and H_2O_2 had opposite effect on oxidative modification of mitochondrial proteins. Carbonylated proteins identified by mass spectrometry are listed in Table 1 (see column titled "H_2O_2 vs young"). Besides proteins identified in fruit under natural senescence, two additional proteins were identified as aconitase (spot 70) and sucrose synthase (spot 74).

Alteration of NADH Oxidation and Mitochondrial Ultrastructure. Using immunological 2D gel electrophoresis followed by MS/MS analysis, mitochondrial VDAC was found to be more oxidized during fruit senescence (Figure 5A). Because carbonylation generally causes protein dysfunction or loss of structural integrity,[31] we analyzed the effect of protein oxidation on function of mitochondrial VDAC. VDAC is a major mitochondrial outer membrane transporter which controls the flux of metabolites such as NADH and ATP across the membrane.[54] When NADH is added externally to the isolated mitochondria, it crosses the mitochondrial outer membrane and is oxidized primarily by an enzyme located on the outer surface of the mitochondrial inner membrane. Since mitochondrial VDAC provides the major pathway by which NADH enters the mitochondria, determining the rate of NADH oxidation can reflect the state and function of VDAC.[49,55] We found that senescent fruit yielded an increased rate of NADH oxidation as indicated by a faster drop in NADH concentration with time (Figure 5B), suggesting an enhanced permeability of these mitochondria to NADH. Similarly, fruit treated with H_2O_2 showed increased rate in NADH oxidation. By comparison, NADH oxidation did not exhibit significant changes in fruit under low temperature. To investigate if VDAC carbonylation leads to permeability transition pore (PTP) opening, which may result in matrix swelling and rupture of the mitochondrial outer membrane, we detected the changes of mitochondrial ultrastructure.

Table 1. Oxidised Mitochondrial Proteins Identified by Tandem Mass Spectrometry

spot	protein name	NCBI accession	theo. M_r (kDa)/pI^a	expt. M_r (kDa)/pI^b	species	Mascot score^c	NP^d	SC (%)^e	senescent vs young ± S.D.^{f}	low temp. vs young ± S.D.^{g}	H_2O_2 vs young ± S.D.^{h}
					Tricarboxylic Acid Cycle-Related						
70	aconitase	gil29027432	98.1/6.07	99/6.6	*Lycopersicon pennellii*	132	3	5	—^{i}	—^{i}	>100^j
51	NAD-dependent malate dehydrogenase	gil15982948	35.5/6.60	39/7.4	*Prunus persica*	389	8	31	>100^j	—^{i}	>100^j
11	NADP-dependent malic enzyme	gil1708924	65.2/6.09	66/6.2	*Vitis vinifera*	383	12	20	4.59 ± 0.91	0.87 ± 0.87	3.41 ± 0.55
14	2-oxoacid dehydrogenase family protein	gil30687411	39.7/6.95	53/6.7	*Arabidopsis thaliana*	141	3	17	2.50 ± 0.54	0.46 ± 0.15	2.84 ± 0.21
12	pyruvate decarboxylase	gil167374781	65.4/5.74	65/6.1	*Prunus armeniaca*	297	10	28	3.17 ± 0.56	2.88 ± 0.24	0.85 ± 0.36
					Membrane Carriers						
47	porin	gil5031279	29.7/7.05	33/8.1	*Prunus armeniaca*	431	9	43	1.28 ± 0.15	0.78 ± 0.78	2.70 ± 0.86
78	porin, putative	gil15229642	24.6/9.19	38/9.1	*Arabidopsis thaliana*	70	1	5	4.33 ± 0.54	2.58 ± 1.08	1.54 ± 0.83
46	mitochrondrial voltage-dependent anion-selective channel	gil67848430	29.7/8.56	37/8.9	*Phaseolus coccineus*	86	5	24	1.77 ± 0.61	0.81 ± 0.81	7.25 ± 2.12
					Heat Shock Protein and Protein Processing						
1	heat shock protein 70	gil6911553	70.8/5.29	71/5.3	*Cucumis sativus*	460	13	25	1.08 ± 0.27	0 ± 0	2.03 ± 0.62
13	mitochondrial processing peptidase	gil13959067	59.2/5.93	57/6.8	*Avicennia marina*	60	3	7	2.22 ± 1.06	2.07 ± 1.09	1.95 ± 0.44
62	mitochondrial ribosomal protein L13	gil159479034	29.7/9.94	21/8.9	*Chlamydomonas reinhardtii*	46	2	2	1.47 ± 0.44	2.56 ± 2.56	3.95 ± 1.19
					Oxidative Stress						
59	superoxide dismutase [Mn], mitochondrial precursor	gil37999810	25.4/8.62	26/6.9	*Prunus persica*	323	7	30	1.64 ± 0.59	1.16 ± 0.83	3.33 ± 1.05
					Carbon and Nitrogen Metabolism						
40	enoyl-CoA hydratase	gil2688820	31.0/7.30	45/8.5	*Prunus armeniaca*	169	3	17	1.88 ± 0.54	0 ± 0	2.04 ± 0.99
37	gamma-aminobutyrate transaminase	gil29837286	57.2/6.72	52/7.1	*Lycopersicon esculentum*	296	6	15	1.27 ± 0.46	10.39 ± 6.70	4.40 ± 1.47
					Miscellaneous Function						
63	glutathione *S*-transferase	gil114795078	23.6/5.42	27/7.4	*Pyrus communis*	111	4	18	1.81 ± 0.59	1.09 ± 1.09	8.25 ± 1.83
83	annexin	gil512400	34.9/5.41	38/6.8	*Medicago sativa*	81	2	5	14.99 ± 4.85	8.80 ± 1.80	5.11 ± 0.51
28	14-3-3 family protein	gil55375985	29.7/4.75	33/5.1	*Malus domestica*	342	8	37	1.33 ± 0.32	0.89 ± 0.24	2.88 ± 1.50
3	hydrogen ion transporting ATP synthase	gil15233891	54.3/5.03	58/5.2	*Arabidopsis thaliana*	832	16	57	1.75 ± 0.67	6.68 ± 1.95	2.55 ± 0.81
86	glyceraldehyde-3-phosphate dehydrogenase	gil145617261	21.5/9.13	39/8.3	*Medicago sativa*	413	6	47	>100^j	>100^j	>100^j
74	sucrose synthase	gil1351138	91.6/6.35	90/6.6	*Alnus glutinosa*	238	10	13	—^{i}	—^{i}	>100^j
94	enolase	gil1169534	47.9/5.56	60/5.9	*Ricinus communis*	367	9	34	3.04 ± 1.27	1.47 ± 0.27	1.62 ± 0.40
					Unknown Function						
41	hypothetical protein	gil147809687	32.7/5.76	37/6.3	*Vitis vinifera*	59	2	10	2.08 ± 1.58	1.43 ± 0.32	2.31 ± 0.65
45	unknown	gil118489666	29.5/8.86	33/9.1	*Populus trichocarpa*	56	1	4	7.83 ± 2.32	7.37 ± 1.22	37.92 ± 6.80
57	hypothetical protein	gil147866185	18.2/6.82	18/7.1	*Vitis vinifera*	141	2	14	>100^j	>100^j	>100^j
77	unknown protein	gil148807158	14.9/6.56	37/9.2	*Prunus dulcis*	418	8	77	3.79 ± 1.97	2.94 ± 1.32	4.11 ± 1.68
53	hypothetical protein	gil147797489	27.3/5.91	29/6.2	*Vitis vinifera*	233	7	35	3.60 ± 0.63	1.86 ± 1.86	5.44 ± 1.74
93	unknown	gil118481885	35.9/6.99	36/7.7	*Populus trichocarpa*	327	7	23	1.39 ± 0.31	0.99 ± 0.99	2.77 ± 0.71
54	ARG10	gil2970051	25.5/5.62	30/6.1	*Vigna radiata*	85	2	13	9.69 ± 1.84	3.03 ± 1.03	13.96 ± 2.48

[a] Theo. M_r (kDa)/p*I*, theoretical molecular mass and isoelectric point based on amino acid sequence of the identified protein. [b] Expt. M_r (kDa)/p*I*, experimental molecular mass and isoelectric point estimated from the 2D gels. [c] Mascot scores greater than 46 are statistically significant ($p < 0.05$). [d] NP, the number of matched peptides. [e] SC, amino acid sequence coverage for the identified proteins. [f] Senescent vs young, average fold change of specific protein carbonylation levels (ratio of spot intensity obtained on the 2D blots over spot intensity on the gels) in senescent fruit versus young fruit from three biological repeats. SD means standard deviation. [g] Low temp. vs young, average fold change of specific protein carbonylation levels in fruit under low temperature versus young fruit from three biological repeats. [h] H_2O_2 vs young, average fold change of specific protein carbonylation levels in fruit treated with H_2O_2 versus young fruit from three biological repeats. [i] The dash (—) means that the accumulation level of the corresponding carbonylated protein in both conditions was close to background. [j] The value >100 means that the accumulation level of the corresponding carbonylated protein in the young fruit was close to background.

Electron microscopy study revealed that the organization of mitochondrial membranes was preserved during natural senescence (Figure 5C). This is consistent with previous observation that mitochondria did not show any breakdown until fruit entered the late stage of senescence.[56] The ultrastructure of mitochondria under low temperature was similar to that in the young fruit. On the other hand, when fruits were treated with H_2O_2, it appeared that the outer membrane was damaged in some mitochondria (Figure 5C).

Detection of MnSOD and Reactive Oxygen Species. As shown in close-up views of the 2D gels and blots (Figure 6A), mitochondrial MnSOD exhibited a significant increase in carbonylation levels in senescent fruit compared to young. We investigated the enzyme activity of MnSOD in purified mitochondria and found that the activity of MnSOD was 46% lower in senescent fruit (Figure 6B). Treatment of fruit with H_2O_2 enhanced the carbonylation levels of MnSOD with reduced enzyme activity. Since MnSOD is the primary antioxidant enzyme that scavenges superoxide radicals (O_2^-) produced in the mitochondria, we hypothesized that decreased catalytic activity of MnSOD caused by oxidative modification would result in the accumulation of O_2^-. To test this, we measured the production of O_2^- in purified mitochondria. In support of our hypothesis, Figure 6C shows that the content of O_2^- in mitochondria of senescent fruit was significantly higher (by about 36%) than that of young fruit. Fruit treated with H_2O_2 showed the highest levels of O_2^-, implying the potential effect of ROS on mitochondrial

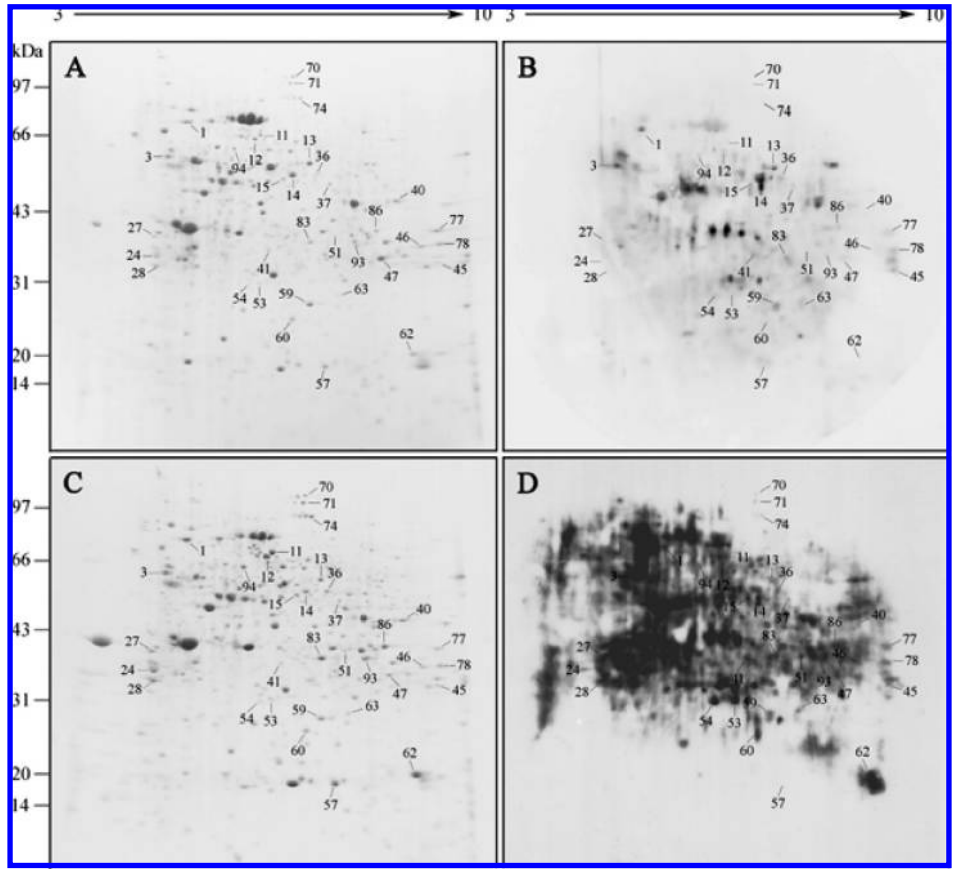

Figure 4. Two-dimensional (2D) immunoblots of carbonylated mitochondrial proteins under low temperature or hydrogen peroxide stress. Mitochondria were isolated from fruit placed under low temperature (A and B) or treated with hydrogen peroxide (C and D). Mitochondrial proteins were separated by 2D gel electrophoresis using 13 cm Immobiline Drystrip with a pH 3−10 nonlinear gradient. After electrophoresis, proteins were visualized by Coomassie blue staining (A and C) or transferred to PVDF membrane for immunoblot analysis with anti-dinitrophenyl-group antibodies (B and D). Those proteins whose levels of carbonylation increased significantly are indicated on both the protein stains and immunoblots. Numbers correspond to the proteins that have been identified by mass spectrometry (listed in Table 1).

antioxidant proteins. In contrast, O_2^- in fruit under low temperature showed no significant difference relative to that of young fruit.

Protein Oxidation Leads to Inactivation of TCA Cycle Enzyme. Generally, oxidative modification of proteins leads to loss of enzyme activity.[32] In this study, we found that the carbonylation levels of mitochondrial malate dehydrogenase increased dramatically during fruit senescence or under H_2O_2 stress (Figure 7A). To assess whether carbonylation of specific enzymes would decrease their catalytic activity, the activity of mitochondrial malate dehydrogenase was estimated. The results indicated a decreased activity of malate dehydrogenase in senescent fruit, but not in fruit under low temperature (Figure 7C). Meanwhile, fruit treated with H_2O_2 showed lower activity of malate dehydrogenase compared to senescent fruit, indicating that oxidative stress could reduce the catalytic activity of this enzyme. Although we did not observe the increase in aconitase carbonylation in senescent fruit, it was detected in fruit treated with H_2O_2 (Figure 7B). Aconitase activity decreased to 76% of that in young fruit, suggesting the negative influence of oxidative stress on this enzyme (Figure 7D).

Discussion

Mitochondria play a critical role in multiple cellular processes, including ATP synthesis, calcium homeostasis, and cell signaling.[57] Since mitochondria are the primary site of generation of ROS such as superoxide anion radical and hydrogen peroxide, oxidative modification of mitochondria components has been implicated during various pathophysiological states associated with oxidative stress and senescent changes.[58] To provide important insight into the role of mitochondrial protein oxidation in the progression of fruit senescence, we have employed high resolution 2D gel electrophoresis coupled with immunoblots using anti-dinitrophenyl-group antibodies to characterize the mitochondrial oxidatively modified proteins. Through ESI-MS/MS, 28 proteins which exhibited an increase in carbonylation were identified (Table 1).

In particular, the carbonylation levels of a mitochondrial outer membrane protein, voltage-dependent anion-selective channel (VDAC, or mitochondrial porin), increased dramatically in senescent or H_2O_2-treated fruit. VDACs, which are highly conserved among eukaryotic cells,[59] are channel-forming proteins that form the major pathway in the mitochondrial outer membrane and control metabolite flux across the membrane.[60] Small metabolites up to 5000 Da could be transported across these membrane-spanning channels in its open configuration.[61,62] The change in the specific modification state of VDAC was likely to be involved in mitochondrial dysfunction.[63] To determine whether protein oxidative modification alters VDAC function, we monitored the permeability of the outer membrane to the metabolite NADH, namely, NADH oxidation,

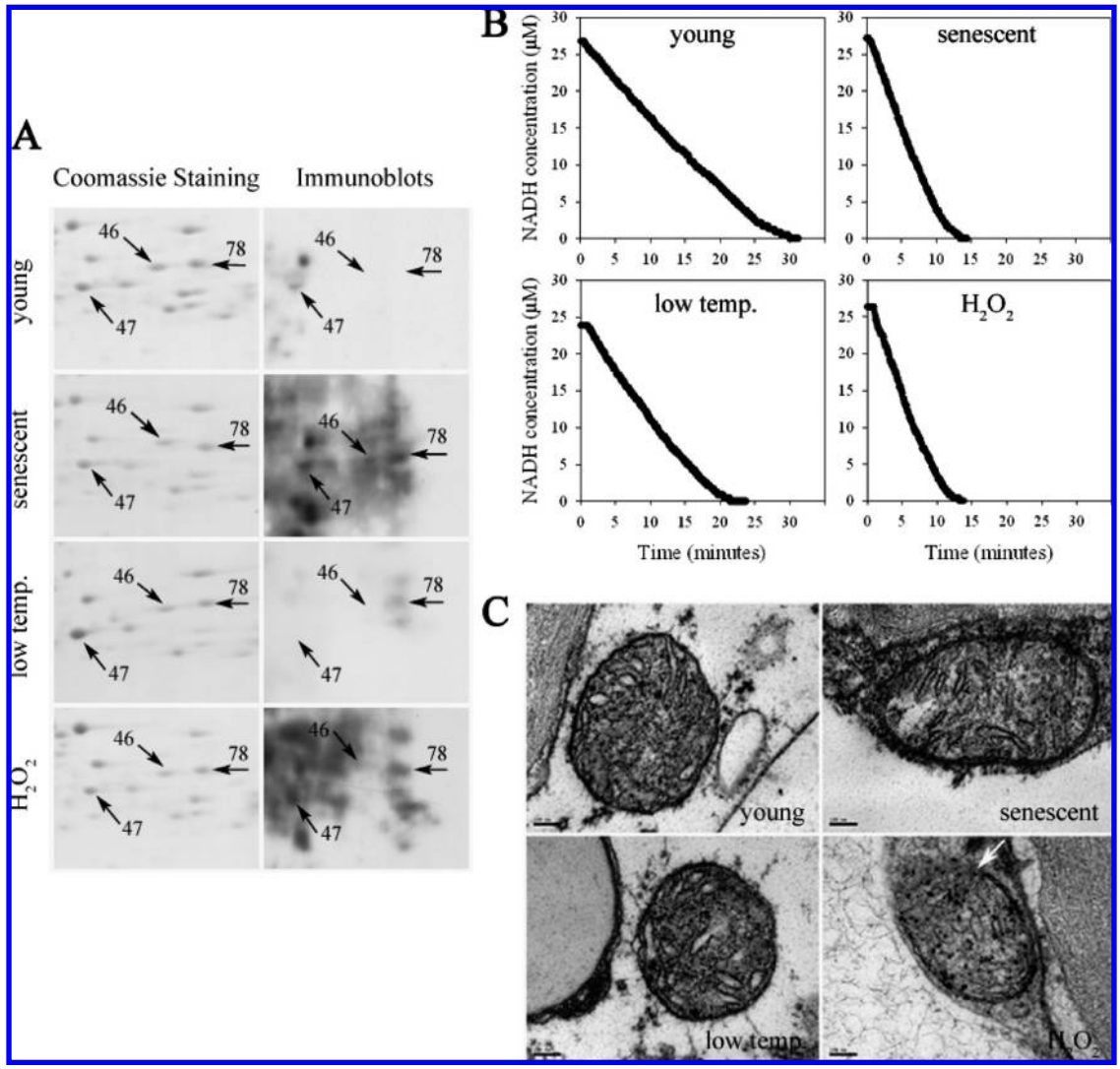

Figure 5. Functional analysis of mitochondrial voltage-dependent anion-selective channel (VDAC). (A) Close-up views of protein carbonylation of mitochondrial VDAC during natural senescence or under conditions of low temperature (low temp.) and experimentally induced oxidative stress. Mitochondrial proteins were separated by 2D gel electrophoresis followed by immunoblots as described in Figures 3 and 4. (B) Measurement of VDAC functions by determining the permeability of mitochondrial outer membrane to metabolite NADH, namely NADH oxidation, using purified mitochondria. The NADH oxidation was monitored by the decrease in absorbance at 340 nm and the absorbance was converted to NADH concentration by dividing it by the molar extinction coefficient (6.22×10^3 mM^{-1} cm^{-1}). (C) Electron microscopy observation of mitochondrial ultrastructure. Arrow points to an example of discontinuity in the outer mitochondrial membrane. The scale bars represent 0.1 μm.

using purified mitochondria. It is reported that determining the rate of NADH oxidation may reflect the state and function of VDAC.[49,55] We found that senescent and H_2O_2-treated fruit yielded an increased rate of NADH oxidation, indicating the changes of VDAC function when carbonylation levels of VADC increased (Figure 5B). By comparison, fruit placed under low temperature, which inhibited the increase of VDAC carbonylation levels, did not show marked increase in NADH oxidation. These results suggest that oxidative modification of VDAC caused by ROS is correlated with the alteration of VDAC function.

VDAC has been linked to the mitochondrial permeability transition pore (PTP), which consists of several proteins, including the adenine nucleotide translocator, the cyclophilin-D, and the VDAC at contact sites between the mitochondrial inner and outer membranes.[64−66] Opening of PTP would result in the swelling of the mitochondrial matrix space and rupture of the outer mitochondrial membrane.[59,65,67] Since VDAC is a component of PTP complex, we propose that the alteration of VDAC function caused by protein carbonylation might trigger PTP opening. Results of transmission electron microscopy showed that VDAC oxidation was paralleled by the damage of outer mitochondrial membrane in fruit treated with H_2O_2 (Figure 5C). Our result is consistent with the finding reported by Shimizu et al.[66] that VDAC dysfunction is essential for mitochondrial permeability transition and thus may directly impair mitochondrial function. Taken together, these data suggest that protein oxidative modification may be associated with the alteration of VDAC function and PTP opening, eventually leading to the mitochondrial dysfunction and fruit senescence.

A noteworthy observation in our study is the specific carbonylation of proteins associated with oxidative stress such as mitochondrial MnSOD and HSP70. As the primary antioxi-

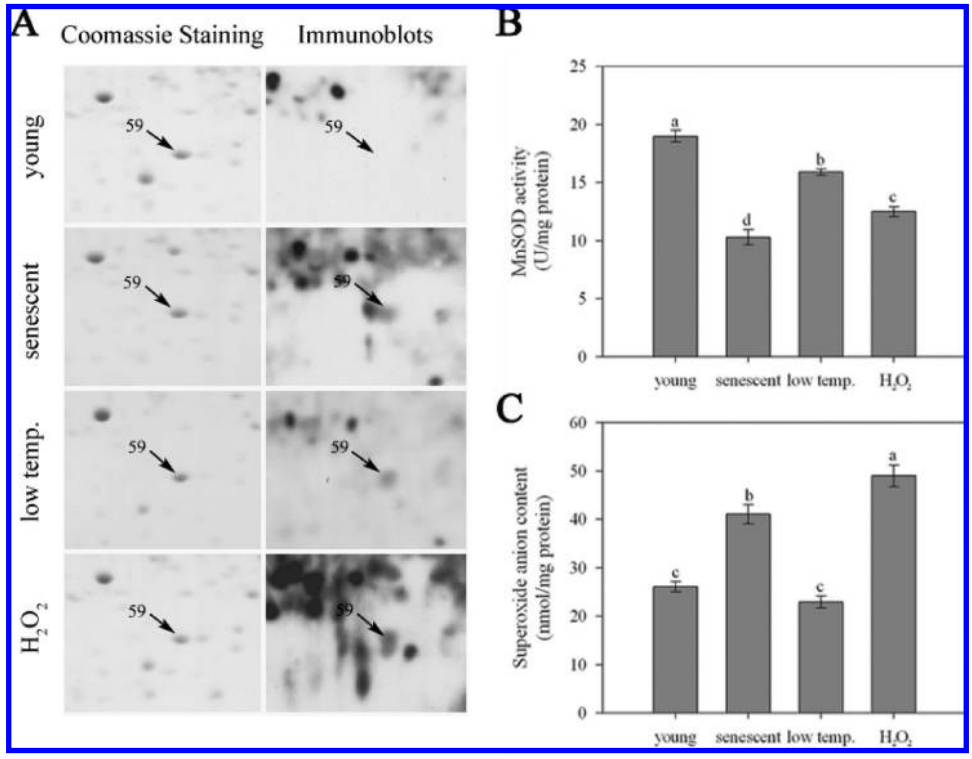

Figure 6. Protein carbonylation reduces enzyme activity of manganese superoxide dismutase (MnSOD) and leads to accumulation of superoxide radicals. (A) Close-up views of protein carbonylation of mitochondrial MnSOD during natural senescence or under conditions of low temperature (low temp.) and experimentally induced oxidative stress. Mitochondrial proteins were separated by 2D gel electrophoresis followed by immunoblots as described in Figures 3 and 4. (B and C) Alteration of MnSOD activity (B) and superoxide radical level (C) after protein carbonylation. The data represent mean ± standard deviation from three different experiments. Bars with different letters are significantly different from each other by the least significant difference test ($p < 0.05$).

dant enzyme that scavenges superoxide radicals produced in the mitochondria, MnSOD has been shown to protect oxygen-utilizing cells from the toxicity of the ROS. It is well-documented that overexpression of MnSOD increases resistance to mitochondrial dysfunction, permeability transition, and apoptotic death invoked by oxidative stress in various disease contexts,[68−71] whereas suppression of MnSOD expression causes specific disturbance of mitochondrial redox homeostasis.[72] In this study, we found an elevation in the amount of MnSOD carbonylation in mitochondria from senescent fruit. This is consistent with the finding reported by Soreghan et al.[30] that MnSOD was subjected to carbonylation during the course of senescence. MnSOD also displays relatively high susceptibility to carbonylation under conditions of experimentally induced oxidative stress (Figure 6A). Since oxidatively modified proteins are generally dysfunctional, losing catalytic activity or structural integrity,[31] it is conceivable that the increase in the carbonylation levels of MnSOD might change its functional properties and thus cause an enhancement of superoxide radicals. As expected, the oxidative damage of MnSOD detected immunochemically was paralleled by a loss of catalytic activity of this antioxidant enzyme (Figure 6B). Meanwhile, content of superoxide radicals increased in mitochondria isolated from senescent and H_2O_2-treated fruit (Figure 6C). In contrast, superoxide radicals showed no significant increase in fruit under low temperature which delayed fruit senescence. Our data indicated that oxidative stress encountered by fruit during senescence process caused the dysfunction of antioxidant enzymes such as MnSOD, which in turn stimulated the accumulation of ROS. The enhanced ROS could increase the carbonylation levels of other proteins which are susceptible to oxidation and eventually lead to fruit senescence.

Another protein whose carbonylation level increased under condition of oxidative stress induced by H_2O_2 is HSP70. Heat shock proteins, also called "molecular chaperones", are a family of proteins whose syntheses are induced when cells are exposed to stress situations including heat shock, exposure to free radicals, and tissue injuries.[73] The specific oxidation of HSP70 is interesting because it was suggested that molecular chaperones act as shields protecting proteins against oxidative damage. In addition, it is thought that molecular chaperones closely interact with misfolded or damaged proteins to assist their refolding.[36] Our result is in agreement with previous reports showing that HSP70 is susceptible to oxidative stress.[36,37] By comparison, protein carbonylation of HSP70 was not observed in fruit under low temperature, which retarded fruit senescence. We suggest here that the specific oxidation of HSP70 may enhance the toxic effect of oxidative stress, thus, leading to further mitochondrial dysfunction.

Impairment of energy metabolism has been shown to contribute to the process of senescence or senescence-associated disorders.[28,31,74] The tricarboxylic acid (TCA) cycle enzymes appear to be particularly susceptible to oxidative damage.[27,31] Inactivation of key components of TCA cycle may block normal electron flow to oxygen and cause an elevation in the amount of ROS, thus, further increasing oxidative damage to macromolecules.[27] Yan et al.[28] demonstrated that oxidative modification of aconitase, an enzyme in the TCA cycle, initiated a cascade with the potential to cause a dramatic increase in the cellular burden of oxidative damage during

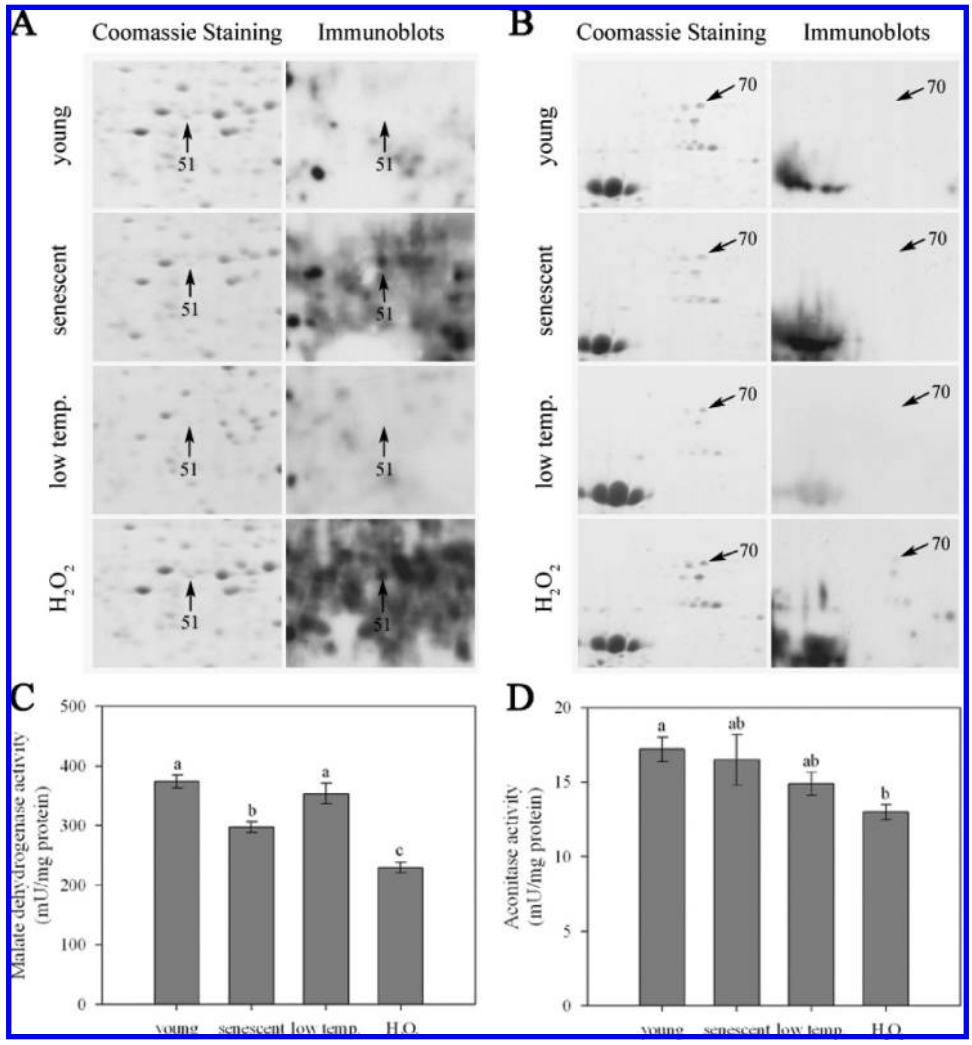

Figure 7. Alteration of catalytic activity of aconitase and malate dehydrogenase after protein carbonylation. (A and B) Close-up views of protein carbonylation of mitochondrial malate dehydrogenase (A) and aconitase (B) during natural senescence or under conditions of low temperature (low temp.) and experimentally induced oxidative stress. Mitochondrial proteins were separated by 2D gel electrophoresis followed by immunoblots as described in Figures 3 and 4. (C and D) Alteration of enzyme activity of malate dehydrogenase (C) and aconitase (D) after protein carbonylation. The data represent mean ± standard deviation from three different experiments. Bars with different letters are significantly different from each other by the least significant difference test ($p < 0.05$).

senescence of housefly. Interestingly, in this study, we found increased carbonylation levels of aconitase under condition of H_2O_2 treatment and malate dehydrogenase during natural senescence. Protein carbonylation resulted in a corresponding loss in catalytic activity of these two enzymes (Figure 7C,D). Aconitase is believed to be particularly sensitive to attacks by superoxide anion radical. This may be related to the iron−sulfur cluster [4Fe−4S] in its active site,[75] which can cause the release of free iron and, in turn, trigger a cascade of oxidative modifications in macromolecules through the Fenton reaction.[76] We propose that the decrease of catalytic activities of aconitase and malate dehydrogenase caused by carbonylation may result in secondary deleterious alterations, leading to an accumulation of ROS. Consistent with the increase in protein carbonylation, improved content of superoxide radicals was observed (Figure 6C). These results indicated a detrimental cycle of mitochondrial protein oxidation, which causes damage to the mitochondria that in turn facilitates further release of ROS, eventually resulting in the mitochondrial dysfunction and cellular senescence. Besides aconitase and malate dehydrogenase, several enzymes involved in energy metabolism such as NADP-dependent malic enzyme, 2-oxoacid dehydrogenase family protein, pyruvate decarboxylase, enoyl-CoA hydratase, and gamma-aminobutyrate transaminase were also identified in our study. The relationship between oxidative damage of these proteins and fruit senescence needs to be further investigated.

We identified two enzymes of glycolysis, glyceraldehyde 3-phosphate dehydrogenase and enolase, which were reported to be highly susceptible to protein oxidation.[31,46,76] It is likely that these two proteins are present in mitochondria or attached to the mitochondrial outer membrane.[77] Alternatively, they may be contaminants from the mitochondrial purification process. Additionally, we identified seven proteins that did not display any significant similarity to proteins with known function in the protein database. Their biological functions on fruit senescence need to be elucidated.

In summary, using functional proteomics or redox proteomics, we have observed enhanced carbonylation levels of mitochondrial proteins including mitochondrial VDAC, MnSOD, and TCA-cycle enzymes in the process of fruit senescence. Increasing the carbonylation levels of mitochondrial proteins

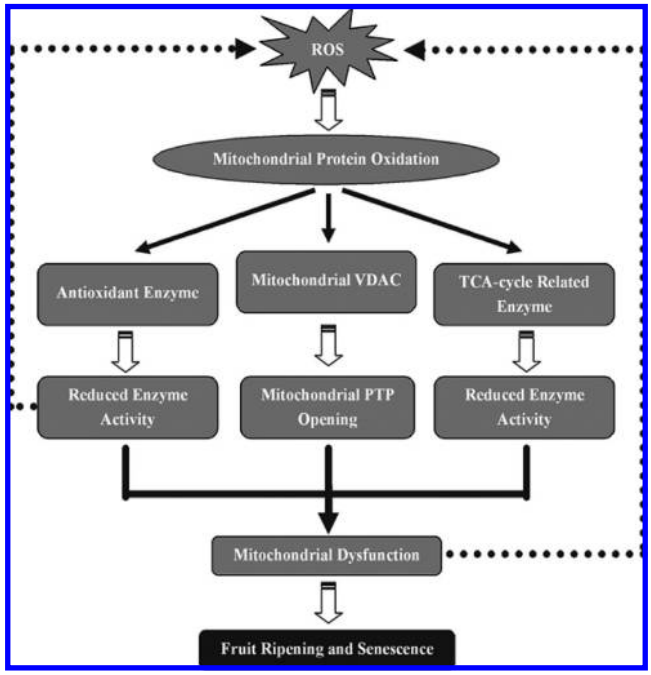

Figure 8. Model for the regulatory effect of mitochondrial protein oxidation on fruit senescence. Accumulation of ROS during fruit senescence increases mitochondrial protein damage. The specific targets of oxidative modification include antioxidant enzyme, mitochondrial voltage-dependent anion-selective channel (VDAC), and tricarboxylic acid (TCA) cycle enzyme. Oxidation of these proteins is paralleled by the loss of catalytic activity of antioxidant protein and TCA cycle enzyme, and alteration of VDAC function. The changes of functional properties of these proteins might in turn facilitate further release of ROS, increasing oxidative damage to mitochondria, and eventually lead to the mitochondrial dysfunction and fruit senescence. PTP, permeability transition pore.

by H_2O_2 treatment accelerated fruit senescence, whereas reducing the carbonylation levels of protein targets by lowering environmental temperature delayed senescence process. Oxidation of these proteins is paralleled by the changes of biological function or loss of enzyme activity. These deleterious alterations caused by protein carbonylation might in turn facilitate further release of ROS, increasing oxidative damage to mitochondria, and eventually lead to the mitochondrial dysfunction and fruit senescence. Model for the regulatory effect of mitochondrial protein oxidation on fruit senescence is proposed in Figure 8. Our results provide the first evidence that carbonylation of specific mitochondrial proteins contributes to fruit senescence. Since ROS have also been implicated in various environmental stresses including ultraviolet radiation, hypoxia, and pathogen attack, our modes of regulation of ROS may also apply to elucidate the roles that ROS play in these processes.

Abbreviations: ROS, reactive oxygen species; 2D, two-dimensional; DNP, 2,4-dinitrophenylhydrazone; DNPH, 2,4-dinitrophenylhydrazine; CBB, Coomassie Brilliant Blue; ESI-MS/MS, electrospray ionization tandem mass spectrometry; MnSOD, manganese superoxide dismutase; TCA cycle, tricarboxylic acid cycle; VDAC, voltage-dependent anion-selective channel; HSP, heat shock protein; PTP, permeability transition pore.

Acknowledgment. This study was supported by the National Natural Science Foundation of China (30430480; 30500351) and the Knowledge Innovation Program of the Chinese Academy of Sciences (110300Q001). We thank Dr. Jun Li for his help in the analysis of MS/MS, Jia Liu for the detection of fruit firmness, and Zhansheng Ding for the determination of hydrogen peroxide. We also thank Dr. Li Li for her valuable suggestions and careful correction of the manuscript.

Supporting Information Available: Supplementary Table 1 shows MS BLAST searches for proteins that were identified with MS/MS spectra matched to less than three peptides. Supplementary Table 2 shows single-peptide-based protein identifications. Supplementary Table 3 shows MS/MS peptide sequence of the identified proteins. Supplementary Figure 1 shows purity evaluation of fruit mitochondria isolated using a two-step Percoll density gradient. Supplementary Figure 2 shows the schematic overview of mitochondrial protein carbonylation analysis used in our study. Supplementary Figure 3 shows the changes of firmness and hydrogen peroxide content in fruit during natural senescence or under low temperature. Supplementary Figure 4 shows the alteration of hydrogen peroxide content and decay development in fruit during natural senescence or treated with hydrogen peroxide. This material is available free of charge via the Internet at http://pubs.acs.org.

References

(1) Manning, K.; Tör, M.; Poole, M.; Hong, Y.; Thompson, A. J.; King, G. J.; Giovannoni, J. J.; Seymour, G. B. A naturally occurring epigenetic mutation in a gene encoding an SBP-box transcription factor inhibits tomato fruit ripening. *Nat. Genet.* **2006**, *38*, 948–952.
(2) Alba, R.; Payton, P.; Fei, Z.; McQuinn, R.; Debbie, P.; Martin, G. B.; Tanksley, S. D.; Giovannoni, J. J. Transcriptome and selected metabolite analyses reveal multiple points of ethylene control during tomato fruit development. *Plant Cell* **2005**, *17*, 2954–2965.
(3) Vrebalov, J.; Ruezinsky, D.; Padmanabhan, V.; White, R.; Medrano, D.; Drake, R.; Schuch, W.; Giovannoni, J. A MADS-box gene necessary for fruit ripening at the tomato ripening-inhibitor (Rin) locus. *Science* **2002**, *296*, 343–346.
(4) Adams-Phillips, L.; Barry, C.; Giovannoni, J. Signal transduction systems regulating fruit ripening. *Trends Plant Sci.* **2004**, *9*, 331–338.
(5) Liu, Y.; Roof, S.; Ye, Z.; Barry, C.; van Tuinen, A.; Vrebalov, J.; Bowler, C.; Giovannoni, J. Manipulation of light signal transduction as a means of modifying fruit nutritional quality in tomato. *Proc. Natl. Acad. Sci. U.S.A.* **2004**, *101*, 9897–9902.
(6) Oeller, P. W.; Lu, M. W.; Taylor, L. P.; Pike, D. A.; Theologis, A. Reversible inhibition of tomato fruit senescence by antisense RNA. *Science* **1991**, *254*, 437–439.
(7) Picton, S.; Barton, S. L.; Bouzayen, M.; Hamilton, A. J.; Grierson, D. Altered fruit ripening and leaf senescence in tomatoes expressing an antisense ethylene-forming enzyme transgene. *Plant J.* **1993**, *3*, 469–481.
(8) Causier, B.; Kieffer, M.; Davies, B. MADS-box genes reach maturity. *Science* **2002**, *296*, 275–276.
(9) Brennan, T.; Frenkel, C. Involvement of hydrogen peroxide in the regulation of senescence in pear. *Plant Physiol.* **1977**, *59*, 411–416.
(10) Lacan, D.; Baccou, J. C. High levels of antioxidant enzymes correlate with delayed senescence in nonnetted muskmelon fruits. *Planta* **1998**, *204*, 377–382.
(11) Jimenez, A.; Creissen, G.; Kular, B.; Firmin, J.; Robinson, S.; Verhoeyen, M.; Mullineaux, P. Changes in oxidative processes and components of the antioxidant system during tomato fruit ripening. *Planta* **2002**, *214*, 751–758.
(12) Harman, D. Ageing: A theory based on free radical and radiation chemistry. *J. Gerontol.* **1956**, *11*, 298–300.
(13) Stadtman, E. R. Protein oxidation and aging. *Science* **1992**, *257*, 1220–1224.
(14) Dufour, E.; Boulay, J.; Rincheval, V.; Sainsard-Chanet, A. A causal link between respiration and senescence in *Podospora anserina*. *Proc. Natl. Acad. Sci. U.S.A.* **2000**, *97*, 4138–4143.

(15) Lee, S. S.; Lee, R. Y.; Fraser, A. G.; Kamath, R. S.; Ahringer, J.; Ruvkun, G. A systematic RNAi screen identifies a critical role for mitochondria in *C. elegans* longevity. *Nat. Genet.* **2003**, *33*, 40–48.
(16) Chan, D. C. Mitochondria: Dynamic organelles in disease, ageing, and development. *Cell* **2006**, *125*, 1241–1252.
(17) Scheckhuber, C. Q.; Erjavec, N.; Tinazli, A.; Hamann, A.; Nyström, T.; Osiewacz, H. D. Reducing mitochondrial fission results in increased life span and fitness of two fungal ageing models. *Nat. Cell Biol.* **2007**, *9*, 99–105.
(18) Heazlewood, J. L.; Tonti-Filippini, J. S.; Gout, A. M.; Day, D. A.; Whelan, J.; Millar, A. H. Experimental analysis of the Arabidopsis mitochondrial proteome highlights signaling and regulatory components, provides assessment of targeting prediction programs, and indicates plant-specific mitochondrial proteins. *Plant Cell* **2004**, *16*, 241–256.
(19) Remmen, H. V.; Richardson, A. Oxidative damage to mitochondria and aging. *Exp. Gerontol.* **2001**, *36*, 957–968.
(20) Balaban, R. S.; Nemoto, S.; Finkel, T. Mitochondria, oxidants, and aging. *Cell* **2005**, *120*, 483–495.
(21) Kujoth, G. C.; Hiona, A.; Pugh, T. D.; Someya, S.; Panzer, K.; Wohlgemuth, S. E.; Hofer, T.; Seo, A. Y.; Sullivan, R.; Jobling, W. A.; Morrow, J. D.; Van Remmen, H.; Sedivy, J. M.; Yamasoba, T.; Tanokura, M.; Weindruch, R.; Leeuwenburgh, C.; Prolla, T. A. Mitochondrial DNA mutations, oxidative stress, and apoptosis in mammalian ageing. *Science* **2005**, *309*, 481–484.
(22) Trifunovic, A.; Hansson, A.; Wredenberg, A.; Rovio, A. T.; Dufour, E.; Khvorostov, I.; Spelbrink, J. N.; Wibom, R.; Jacobs, H. T.; Larsson, N. G. Somatic mtDNA mutations cause ageing phenotypes without affecting reactive oxygen species production. *Proc. Natl. Acad. Sci. U.S.A.* **2005**, *102*, 17993–17998.
(23) Bender, A.; Krishnan, K. J.; Morris, C. M.; Taylor, G. A.; Reeve, A. K.; Perry, R. H.; Jaros, E.; Hersheson, J. S.; Betts, J.; Klopstock, T.; Taylor, R. W.; Turnbull, D. M. High levels of mitochondrial DNA deletions in substantia nigra neurons in ageing and Parkinson disease. *Nat. Genet.* **2006**, *38*, 515–517.
(24) Kraytsberg, Y.; Kudryavtseva, E.; McKee, A. C.; Geula, C.; Kowall, N. W.; Khrapko, K. Mitochondrial DNA deletions are abundant and cause functional impairment in aged human substantia nigra neurons. *Nat. Genet.* **2006**, *38*, 518–520.
(25) Groebe, K.; Krause, F.; Kunstmann, B.; Unterluggauer, H.; Reifschneider, N. H.; Scheckhuber, C. Q.; Sastri, C.; Stegmann, W.; Wozny, W.; Schwall, G. P.; Poznanović, S.; Dencher, N. A.; Jansen-Dürr, P.; Osiewacz, H. Z.; Schrattenholz, A. Differential proteomic profiling of mitochondria from *Podospora anserina*, rat and human reveals distinct patterns of age-related oxidative changes. *Exp. Gerontol.* **2007**, *42*, 887–898.
(26) Yan, L. J.; Sohal, R. S. Mitochondrial adenine nucleotide translocase is modified oxidatively during aging. *Proc. Natl. Acad. Sci. U.S.A.* **1998**, *95*, 12896–12901.
(27) Das, N.; Levine, R. L.; Orr, W. C.; Sohal, R. S. Selectivity of protein oxidative damage during aging in *Drosophila melanogaster*. *Biochem. J.* **2001**, *360*, 209–216.
(28) Yan, L. J.; Levine, R. L.; Sohal, R. S. Oxidative damage during aging targets mitochondrial aconitase. *Proc. Natl. Acad. Sci. U.S.A.* **1997**, *94*, 11168–11172.
(29) Bulteau, A.; Szweda, L. I.; Friguet, B. Mitochondrial protein oxidation and degradation in response to oxidative stress and aging. *Exp. Gerontol.* **2006**, *41*, 653–657.
(30) Soreghan, B. A.; Yang, F.; Thomas, S. N.; Hsu, J.; Yang, A. J. High-throughput proteomic-based identification of oxidatively induced protein carbonylation in mouse brain. *Pharm. Res.* **2003**, *20*, 1713–1720.
(31) Perluigi, M.; Poon, H. F.; Maragos, W.; Pierce, W. M.; Klein, J. B.; Calabrese, V.; Cini, C.; De Marco, C.; Butterfield, D. A. Proteomic analysis of protein expression and oxidative modification in R6/2 transgenic mice: A model of Huntington disease. *Mol. Cell. Proteomics* **2005**, *4*, 1849–1861.
(32) Sultana, R.; Boyd-Kimball, D.; Poona, H. F.; Cai, J.; Pierce, W. M.; Klein, J. B.; Markesbery, W. R.; Zhou, X. Z.; Lu, K. P.; Butterfield, D. A. Oxidative modification and down-regulation of Pin1 in Alzheimer's disease hippocampus: A redox proteomics analysis. *Neurobiol. Aging* **2006**, *27*, 918–925.
(33) Oracz, K.; Bouteau, H. E.; Farrant, J. M.; Cooper, K.; Belghazi, M.; Job, C.; Job, D.; Corbineau, F.; Bailly, C. ROS production and protein oxidation as a novel mechanism for seed dormancy alleviation. *Plant J.* **2007**, *50*, 452–465.
(34) Nyström, T. Role of oxidative carbonylation in protein quality control and senescence. *EMBO J.* **2005**, *24*, 1311–1317.
(35) England, K.; O'Driscoll, C.; Cotter, T. G. Carbonylation of glycolytic proteins is a key response to drug-induced oxidative stress and apoptosis. *Cell Death Differ.* **2004**, *11*, 252–260.
(36) Magi, B.; Ettorre, A.; Liberatori, S.; Bini, L.; Andreassi, M.; Frosali, S.; Neri, P.; Pallini, V.; Di Stefano, A. Selectivity of protein carbonylation in the apoptotic response to oxidative stress associated with photodynamic therapy: A cell biochemical and proteomic investigation. *Cell Death Differ.* **2004**, *11*, 842–852.
(37) Kristensen, B. K.; Askerlund, P.; Bykova, N. V.; Egsgaard, H.; Møller, I. M. Identification of oxidised proteins in the matrix of rice leaf mitochondria by immunoprecipitation and two-dimensional liquid chromatography-tandem mass spectrometry. *Phytochemistry* **2004**, *65*, 1839–1851.
(38) Moreau, F.; Romani, R. Preparation of avocado mitochondria using self-generated Percoll density gradients and changes in buoyant density during ripening. *Plant Physiol.* **1982**, *70*, 1380–1384.
(39) Taylor, N. L.; Heazlewood, J. L.; Day, D. A.; Millar, A. H. Differential impact of environmental stresses on the pea mitochondrial proteome. *Mol. Cell. Proteomics* **2005**, *4*, 1122–1133.
(40) Millar, A. H.; Sweetlove, L. J.; Giegé, P.; Leaver, C. J. Analysis of the Arabidopsis mitochondrial proteome. *Plant Physiol.* **2001**, *127*, 1711–1727.
(41) Cantu, D.; Vicente, A. R.; Greve, L. C.; Dewey, F. M.; Bennett, A. B.; Labavitch, J. M.; Powell, A. L. T. The intersection between cell wall disassembly, ripening, and fruit susceptibility to *Botrytis cinerea*. *Proc. Natl. Acad. Sci. U.S.A.* **2008**, *105*, 859–864.
(42) Ding, Z.; Tian, S.; Zheng, X.; Zhou, Z.; Xu, Y. Responses of reactive oxygen metabolism and quality in mango fruit to exogenous oxalic acid or salicylic acid under chilling temperature stress. *Physiol. Plantarum* **2007**, *130*, 112–121.
(43) Wang, Y.; Tian, S.; Xu, Y. Effects of high oxygen concentration on pro- and anti-oxidant enzymes in peach fruits during postharvest periods. *Food Chem.* **2005**, *91*, 99–104.
(44) Manganaris, G. A.; Vasilakakis, M.; Mignani, I.; Manganaris, A. Cell wall physicochemical properties as indicators of peach quality during fruit ripening after cold storage. *Food Sci. Technol. Int.* **2008**, *14*, 385–391.
(45) Bradford, M. M. A rapid and sensitive method for the quantitation of microgram quantities of protein utilizing the principle of protein-dye binding. *Anal. Biochem.* **1976**, *72*, 248–254.
(46) Dirmeier, R.; O'Brien, K. M.; Engle, M.; Dodd, A.; Spears, E.; Poyton, R. O. Exposure of yeast cells to anoxia induces transient oxidative stress. *J. Biol. Chem.* **2002**, *277*, 34773–34784.
(47) Qin, G.; Tian, S.; Chan, Z.; Li, B. Crucial role of antioxidant proteins and hydrolytic enzymes in pathogenicity of *Penicillium expansum:* Analysis based on proteomic approach. *Mol. Cell. Proteomics* **2007**, *6*, 425–438.
(48) Shevchenko, A.; Sunyaev, S.; Loboda, A.; Shevchenko, A.; Bork, P.; Ens, W.; Standing, K. G. Charting the proteomes of organisms with unsequenced genomes by MALDI-Quadrupole Time-of-Flight mass spectrometry and BLAST homology searching. *Anal. Chem.* **2001**, *73*, 1917–1926.
(49) Yagoda, N.; von Rechenberg, M.; Zaganjor, E.; Bauer, A. J.; Yang, W. S.; Fridman, D. J.; Wolpaw, A. J.; Smukste, I.; Peltier, J. M.; Boniface, J. J.; Smith, R.; Lessnick, S. L.; Sahasrabudhe, S.; Stockwell, B. R. RAS-RAF-MEK-dependent oxidative cell death involving voltage-dependent anion channels. *Nature (London)* **2007**, *447*, 864–868.
(50) Jakubowski, W.; Biliński, T.; Bartosz, G. Oxidative stress during aging of stationary cultures of the yeast Saccharomyces cerevisiae. *Free Radical Biol. Med.* **2000**, *28*, 659–664.
(51) Minotti, G.; Recalcati, S.; Mordente, A.; Liberi, G.; Calafiore, A. M.; Mancuso, C.; Preziosi, P.; Cairo, G. The secondary alcohol metabolite of doxorubicin irreversibly inactivates aconitase/iron regulatory protein-1 in cytosolic fractions from human myocardium. *FASEB J.* **1998**, *12*, 541–552.
(52) Pierpoint, W. S. The distribution of succinate dehydrogenase and malate dehydrogenase among components of tobacco-leaf extracts. *Biochem. J.* **1963**, *88*, 120–125.
(53) O'Brien, K. M.; Dirmeier, R.; Engle, M.; Poyton, R. O. Mitochondrial protein oxidation in yeast mutants lacking manganese- (MnSOD) or copper- and Zinc-containing superoxide dismutase (CuZnSOD). *J. Biol. Chem.* **2004**, *279*, 51817–51827.
(54) Abu-Hamad, S.; Sivan, S.; Shoshan-Barmatz, V. The expression level of the voltage-dependent anion channel controls life and death of the cell. *Proc. Natl. Acad. Sci. U.S.A.* **2006**, *103*, 5787–5792.
(55) Lee, A. C.; Xu, X.; Blachly-Dyson, E.; Forte, M.; Colombini, M. The role of yeast VDAC genes on the permeability of the mitochondrial outer membrane. *J. Membr. Biol.* **1998**, *161*, 173–181.
(56) Biale, J. B. Growth, maturation, and senescence in fruits. *Science* **1964**, *146*, 880–888.
(57) Brown, G. C. Control of respiration and ATP synthesis in mammalian mitochondria and cells. *Biochem. J.* **1992**, *284*, 1–13.

(58) Toroser, D.; Orr, W. C.; Sohal, R. S. Carbonylation of mitochondrial proteins in *Drosophila melanogaster* during aging. *Biochem. Biophys. Res. Commun.* **2007**, *363*, 418–424.
(59) Colombini, M. VDAC: The channel at the interface between mitochondria and the cytosol. *Mol. Cell. Biochem.* **2004**, *256/257*, 107–115.
(60) Lemasters, J. J.; Holmuhamedov, E. Voltage-dependent anion channel (VDAC) as mitochondrial governator-Thinking outside the box. *Biochim. Biophys. Acta* **2006**, *1762*, 181–190.
(61) Harris, M. H.; Thompson, C. B. The role of the Bcl-2 family in the regulation of outer mitochondrial membrane permeability. *Cell Death Differ.* **2000**, *7*, 1182–1191.
(62) Vander Heiden, M. G.; Chandel, N. S.; Li, X. X.; Schumacker, P. T.; Colombini, M.; Thompson, C. B. Outer mitochondrial membrane permeability can regulate coupled respiration and cell survival. *Proc. Natl. Acad. Sci. U.S.A.* **2000**, *97*, 4666–4671.
(63) Fukada, K.; Zhang, F.; Vien, A.; Cashman, N. R.; Zhu, H. Mitochondrial proteomic analysis of a cell line model of familial amyotrophic lateral sclerosis. *Mol. Cell. Proteomics* **2004**, *3*, 1211–1223.
(64) McEnery, M. W.; Snowman, A. M.; Trifiletti, R. R.; Snyder, S. H. Isolation of the mitochondrial benzodiazepine receptor: Association with the voltage-dependent anion channel and the adenine nucleotide carrier. *Proc. Natl. Acad. Sci. U.S.A.* **1992**, *89*, 3170–3174.
(65) Madesh, M.; Hajnóczky, G. VDAC-dependent permeabilization of the outer mitochondrial membrane by superoxide induces rapid and massive cytochrome c release. *J. Cell Biol.* **2001**, *155*, 1003–1015.
(66) Shimizu, S.; Matsuoka, Y.; Shinohara, Y.; Yoneda, Y.; Tsujimoto, Y. Essential role of voltage-dependent anion channel in various forms of apoptosis in mammalian cells. *J. Cell Biol.* **2001**, *152*, 237–250.
(67) Vander Heiden, M. G.; Chandel, N. S.; Williamson, E. K.; Schumacker, P. T.; Thompson, C. B. Bcl-x_L regulates the membrane potential and volume homeostasis of mitochondria. *Cell* **1997**, *91*, 627–637.
(68) Klivenyi, P.; St. Clair, D.; Wermer, M.; Yen, H. C.; Oberley, T.; Yang, L.; Beal, M. F. Manganese superoxide dismutase overexpression attenuates MPTP toxicity. *Neurobiol. Dis.* **1998**, *5*, 253–258.
(69) Callio, J.; Oury, T. D.; Chu, C. T. Manganese superoxide dismutase protects against 6-hydroxydopamine injury in mouse brains. *J. Biol. Chem.* **2005**, *280*, 18536–18542.
(70) Silva, J. P.; Shabalina, I. G.; Dufour, E.; Petrovic, N.; Backlund, E. C.; Hultenby, K.; Wibom, R.; Nedergaard, J.; Cannon, B.; Larsson, N. G. SOD2 overexpression: Enhanced mitochondrial tolerance but absence of effect on UCP activity. *EMBO J.* **2005**, *24*, 4061–4070.
(71) Kowluru, R. A.; Kowluru, V.; Xiong, Y.; Ho, Y. S. Overexpression of mitochondrial superoxide dismutase in mice protects the retina from diabetes-induced oxidative stress. *Free Radical Biol. Med.* **2006**, *41*, 1191–1196.
(72) Morgan, M. J.; Lehmann, M.; Schwarzländer, M.; Baxter, C. J.; Sienkiewicz-Porzucek, A.; Williams, T. C. R.; Schauer, N.; Fernie, A. R.; Fricker, M. D.; Ratcliffe, R. G.; Sweetlove, L. J.; Finkemeier, I. Decrease in manganese superoxide dismutase leads to reduced root growth and affects tricarboxylic acid cycle flux and mitochondrial redox homeostasis. *Plant Physiol.* **2008**, *147*, 101–114.
(73) Cabiscol, E.; Bellí, G.; Tamarit, J.; Echave, P.; Herrero, E.; Ros, J. Mitochondrial Hsp60, resistance to oxidative stress, and the labile iron pool are closely connected in *Saccharomyces cerevisiae*. *J. Biol. Chem.* **2002**, *277*, 44531–44538.
(74) Sultana, R.; Boyd-Kimball, D.; Poona, H. F.; Cai, J.; Pierce, W. M.; Klein, J. B.; Merchant, M.; Markesbery, W. R.; Butterfield, D. A. Redox proteomics identification of oxidized proteins in Alzheimer's disease hippocampus and cerebellum: An approach to understand pathological and biochemical alterations in AD. *Neurobiol. Aging* **2006**, *27*, 1564–1576.
(75) Kent, T. A.; Dreyer, J. L.; Kennedy, M. C.; Huynh, B. H.; Emptage, M. H.; Beinert, H.; Münck, E. Mössbauer studies of beef heart aconitase: Evidence for facile interconversions of iron-sulfur clusters. *Proc. Natl. Acad. Sci. U.S.A.* **1982**, *79*, 1096–1100.
(76) Job, C.; Rajjou, L.; Lovigny, Y.; Belghazi, M.; Job, D. Patterns of protein oxidation in Arabidopsis seeds and during germination. *Plant Physiol.* **2005**, *138*, 790–802.
(77) Graham, J. W. A.; Williams, T. C. R.; Morgan, M.; Fernie, A. R.; Ratcliffe, R. G.; Sweetlove, L. J. Glycolytic enzymes associate dynamically with mitochondria in response to respiratory demand and support substrate channeling. *Plant Cell* **2007**, *19*, 3723–3738.

PR801046M